CHEMISTRY
A EUROPEAN JOURNAL

DOI: 10.1002/chem.200500884

A Novel Method for Time-Resolved Fluorimetric Determination and Imaging of the Activity of Peroxidase, and Its Application to an Enzyme-Linked Immunosorbent Assay

Zhihong Lin, Meng Wu, Otto S. Wolfbeis, and Michael Schäferling*[a]

Abstract: A new type of fluorescence assay for the determination of peroxidase (POx) activity is presented. The assay is based on the indication of the enzymatic consumption of H_2O_2 (HP), using a fluorescent europium–tetracycline (Eu_3TC) complex as indicator. On addition of HP, this complex forms a highly fluorescent adduct (Eu_3TC–HP), which is decomposed in the presence of POx to form the weakly fluorescent europium–tetracycline (Eu_3TC). Hence, the activity of the enzyme can be directly determined by means of the luminescent Eu_3TC complex as indicator. The POx assay demonstrated herein was elaborated starting from a spectral characterization of the complex systems involved. Due to the long lifetime of lanthanide luminescence, both steady-state and time-resolved luminescence assays can easily be performed. The time-resolved assay can quantify POx in the range from 4.0×10^{-5} to 5.9×10^{-3} U mL^{-1}, with a limit of detection of 1.0×10^{-5} U mL^{-1}. The effects of POx inhibitors such as cyanide, hydroxylamine, and azide have also been studied. In addition, a time-resolved fluorescent detection method for a POx-based enzyme-linked immunosorbent assay (ELISA) has been developed, which is demonstrated in a sandwich model assay with bovine IgG serving as analyte. Furthermore, a time-resolved fluorescent imaging method is demonstrated that makes use of a straightforward imaging set-up adjusted to the optical properties of the europium reagent.

Keywords: fluorescent probes · imaging agents · immunoassays · peroxidase activity · time-resolved spectrometry

Introduction

Lanthanide-ligand complexes (LLCs) represent an extremely versatile class of compounds because of their large number of coordination sites (up to ten), which have strongly varying affinities for ligands. The trivalent ions Eu^{3+}, Tb^{3+}, and Sm^{3+} are particularly interesting because most of their metal-ligand complexes display luminescence at room temperature, which results from rather complex electronic transitions. This luminescence (to which we and others also refer to as fluorescence) has a long decay time, which can range from several microseconds (μs) to several milliseconds (ms). Among the numerous metal–ligand complexes, those derived from lanthanides have probably exhibited the most diverse range of applications. In many of these LLCs, the organic ligand acts as an antenna that absorbs photonic energy, which is then transfered to the central metal ion.[1–3] Energy level diagrams for all trivalent lanthanide ions have recently been established.[4]

LLCs have been used as luminescent probes for numerous cations (e.g., heavy metal ions)[5,6] and anions,[7–10] as well as for neutral species such as hydrogen peroxide.[11] This is mainly due to the strongly differing binding strengths of various ligands to the sixth and/or ninth binding sites of species such as Eu^{3+}, which makes the intrinsic fluorescence of LLCs hypersensitive to certain ligands. A huge field of (even commercial) application is in (bio)analysis, where LLCs serve as covalent labels, such as for enzyme detection or nucleic acid hybridization assays using the enzyme-amplified lanthanide luminescence (EALL)[12,13] method. So-called dissociation-enhanced lanthanide fluorescence immunoassay (DELFIA) has found numerous applications in immunodiagnostics.[14] A particular feature of LLCs is the long decay time of their luminescence. This has been exploited in both time-resolved and lifetime-based (immuno)assays.[15–17] The fluorescence enhancement of europium complexes with ligands such as tetracycline or metacycline after coordination to specific biomolecules has been used for the determi-

[a] Dr. Z. Lin, Dr. M. Wu, Prof. Dr. O. S. Wolfbeis, Dr. M. Schäferling
Institute of Analytical Chemistry, Chemo- and Biosensors
University of Regensburg, 93040 Regensburg (Germany)
Fax: (+49) 941-943-4064
E-mail: michael.schaeferling@chemie.uni-regensburg.de

nation of DNA[18,19] and proteins such as BSA or lysozyme.[20,21]

Based on previous results by Schulman et al.,[22] we have demonstrated that the europium–tetracycline complex has a binding site that is hypersensitive to the presence of hydrogen peroxide (HP), using europium and tetracycline in a molar ratio of 3:1 (Eu_3TC).[11] This effect can be used not only to sense and image hydrogen peroxide,[23] but also to detect the activity of the enzymes glucose oxidase[24] and catalase.[25] HP binds to the ninth coordination site of Eu_3Tc, thus displacing quenching water molecules and thereby increasing its fluorescence intensity (and lifetime). Moreover, the average decay times of the emissions of Eu_3TC and Eu_3TC–HP differ greatly.

Quite a variety of methods are known for the determination of the activity of peroxidase (POx).[26,27] Almost all are based on the fact that POx reacts with hydrogen peroxide and a second substrate. These second substrates act as hydrogen donors and form complex product mixtures by (re)-combination of radical intermediates. Some of these products are suitable for chromogenic, fluorogenic or other signal-generating purposes. As a result, kinetic assays have been developed based on spectrophotometry/reflectometry,[28,29] fluorimetry,[30,31] chemiluminescence,[32–34] electrochemiluminescence,[35] and electroanalysis.[36,37] Among the fluorimetric methods, those based on time-resolution[38] (often referred to as time-resolved or gated assays) are the most sensitive tools in biological assays. Surprisingly, there has been only one report[39] on the application of time-resolved lanthanide luminescence (using Tb^{3+}), although it is a particularly attractive scheme for the determination of the activity of POx.

The association of hydrogen peroxide (HP) with Eu_3TC is best described by Equation (1),

$$Eu_3TC + n\,H_2O_2 \rightleftharpoons Eu_3TC-HP + (n-1)\,H_2O_2 \qquad (1)$$

which reflects the facts that: a) excess HP is needed to drive the reaction to the right-hand side, and b) on consumption of free HP the equilibrium is shifted back to the left-hand side. We can then make use of the rather surprising fact that the ligation of HP is highly reversible. Changes in this equilibrium result in a very sensitive response of the lanthanide luminescence. These properties suggest that Eu_3TC–HP may be used for a straightforward quantification of the activity of POx. Furthermore, POxs are known for being tolerant to relatively harsh conditions and are therefore among the preferred enzyme labels in enzyme-linked immunosorbent assays (ELISA),[40] nucleic acid assays,[41] in high-throughput screening (HTS),[42] and in histochemical staining and imaging.[43] Thus, the above-mentioned findings led to a new type of time-resolved detection method for ELISAs, with direct visualization by means of a fluorescent imaging device adjusted to the read-out of micro-well plate-based europium luminescence assays.

Results and Discussion

The lanthanide complex as an indicator for HP: The easily accessible probe Eu_3TC is capable of sensing hydrogen peroxide (HP) because on exposure to the latter it undergoes a large increase in fluorescence intensity and a significant change in the pattern of fluorescence decay times.[23] (*Note*: we use the term fluorescence for convenience and by analogy with other authors working with "fluorescent" europium complexes, even though it is known that the emission of such complexes does not occur from a singlet excited state.) The largest signal increase was found for an Eu:TC molar ratio of 3:1. Fluorescence reached a maximum on increasing the concentration of HP from zero to 1.5 mmol L^{-1}. The largest signal increase was found for a solution containing 20 μL of 5 mmol L^{-1} HP and 50 μL of the Eu_3TC stock solution in a total volume of 250 μL, and this composition was used in most experiments.

Owing to the spatial proximity of ligand and Eu^{3+} ions, an efficient ligand-to-metal energy transfer can take place. The residual binding sites and coordination spheres of the Eu^{3+} ions are occupied by water molecules, which act as quenchers (the quantum yield of the Eu_3TC complex in aqueous solution is only 0.3 %). Hydrogen peroxide, being a better coordinating species than water but a weaker quencher, can replace water molecules, and this leads to an increase in quantum yield to about 4.5 %. However, it is likely that the complex binding of Eu^{3+} to TC is rather weak, as has been suggested by others.[44,45] Unfortunately, the complex is only stable in solution and all attempts to isolate crystals of Eu_3TC (in order to perform X-ray analysis) failed.

The detection scheme: It is found that the equilibrium between Eu_3TC and HP on the one side and Eu_3TC–HP on the other [see Eq. (1)] can be readily shifted to the left-hand side (i.e., to Eu_3TC) by peroxidase-catalyzed decomposition of HP. Hence, the reagent, which is easy to prepare, is highly promising as an indicator probe for kinetic assays of the enzymatic activity of POx. Furthermore, the effect of potential activators and inhibitors can be screened. The detection scheme is based on the reverse reaction given in Equation (2).

$$\underset{\text{strong fluorescence}}{Eu_3TC-HP} \xrightarrow{(POx)} \underset{\text{weak fluorescence}}{Eu_3TC} \qquad (2)$$

As pointed out in Equation (1), Eu_3TC–HP is only stable in the presence of an excess of HP, which is the species consumed in the enzymatic reaction. As a result, the equilibrium shown in Equation (2) is shifted to the right-hand side.

Numerous second substrates have been used in POx assays. We use phenol because it is readily available, stable, does not absorb at the wavelengths that can be applied for the excitation of Eu_3TC–HP (370–410 nm), and does not give interfering fluorescent products on oxidation. In a system composed of Eu_3TC–HP, POx, and phenol, the activity of POx is proportional to the decrease in fluorescence

expressed as $\Delta F\,min^{-1}$, where ΔF is the difference between the initial fluorescence intensity (F_0) and the final fluorescence intensity (F), ideally both corrected for a (conceivable) background. Emission can only be detected if the sample is excited with light of a wavelength between 350 and 440 nm (thus excluding the possibility of chemiluminescence).[22,34,45] In the complete absence of phenol, POx does not cause the fluorescence intensity to decrease. If POx is denatured by heating, none of the kinetic effects associated with the presence of active POx are observed.

Kinetic studies: As shown in Figure 1, the activity of POx is directly related to the change in fluorescence intensity of the Eu_3TC–HP system. In the absence of POx (curve A), only small changes are observed, which can be ascribed to temperature effects. As the activity of the POx is increased on going from B to F, the slope increases as well, and this can be used to determine the POx activity. Curve G is a time trace of a system to which no H_2O_2 and no POx were added (i.e., that of pristine Eu_3TC). One needs to keep in mind that in the assay described here, fluorescence does not drop to zero but only from the level of the fluorescence of Eu_3TC–HP to that of Eu_3TC. Once formed, Eu_3TC is not affected by POx. Incubation at elevated temperature accelerates the reaction, so that the fluorescence intensity changes more rapidly. Therefore, even lower activities of POx may be detected at higher temperatures (such as 40–50 °C). The dynamic range of the determination may also be adjusted by regulation of the incubation time.

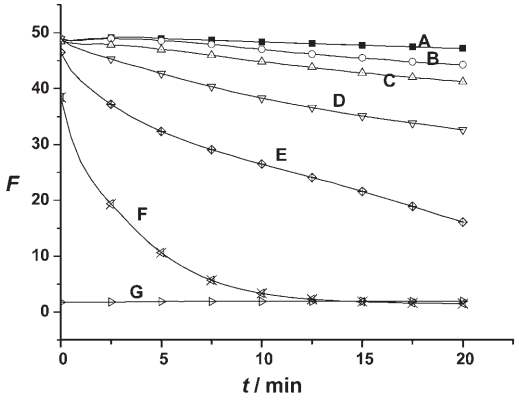

Figure 1. Kinetic analysis of the decomposition of the Eu_3TC–HP complex by POx and phenol as monitored by means of fluorescence: A) after addition of phenol in the absence of POx (50 μL of stock solution of Eu_3Tc, 20 μL of 4 mmol L^{-1} H_2O_2, and 17 μL of 49 mmol L^{-1} phenol, diluted with MOPS to a total volume of 250 μL); B) to F) kinetic traces in the presence of phenol and of 7.6, 22, 76, 220, and 760 mU mL^{-1}, respectively, of POx; (G) no H_2O_2 and POx were added (Eu_3TC signal).

Figure 2 shows the change in the profiles of the fluorescence decay of Eu_3TC on addition of increasing concentrations of HP (curves E to A), recorded by means of the time-correlated single-photon counting (TCSPC) technique. Eu_3TC and Eu_3TC–HP have rather different decay patterns and decay times. An analysis of the decay times of Eu_3TC and Eu_3TC–HP[11,24,49] has revealed that the decay of Eu_3TC–HP can be fitted by a three-component model. The respective decay times are 10 μs (relative amplitude 17 %), 34 μs (18 %), and 61 μs (65 %). The weighted average decay time is 60 μs. For Eu_3TC, the decay times are 7 μs (40 %), 24 μs (54 %), and 53 μs (6 %), the average decay time therefore being much shorter (30 μs). From these results, it is obvious that time-resolved measurements are best performed with a lag time of 60 μs in order to selectively detect the more strongly fluorescent Eu_3TC–HP complex and to minimize the background caused by Eu_3TC as well as by background fluorescences resulting from proteins and plates.

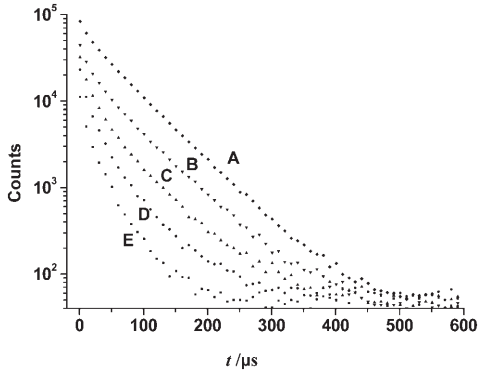

Figure 2. Effect of different H_2O_2 concentrations on the time trace of the decay of the fluorescence intensity of Eu_3TC–HP recorded by TCSPC. From A) to E), the concentrations of H_2O_2 decrease from 300 to 60, 30, 12, and 0 μmol L^{-1}, respectively. All solutions contain 500 μL of Eu_3TC stock solution in a total volume of 2 mL.

Spectral characterization: The excitation and emission spectra of Eu_3TC–HP and Eu_3TC have been reported previously.[11] As in other lanthanide complexes, the photonic energy absorbed by the ligand (TC) in the Eu_3TC complex is transferred to the central Eu^{3+} ion, with its typical emission[44,47] in the form of a main line ($^5D_0 \rightarrow {}^7F_2$) with peaks at 613 and 618 nm (two peaks) and several side bands. The appearance of two main peaks is a clear indication of the change of the ligand field[48] around the Eu^{3+}. From the findings presented so far, we conclude that hydrogen peroxide (HP), on addition to Eu_3TC, replaces at least one water molecule ligated to the Eu^{3+}. On addition of excess HP (i.e., after complete formation of the Eu_3TC–HP complex), the intensity of the emission is higher by a factor of 15. The spectrum of Eu_3TC–HP does not change significantly on addition of phenol alone.

Effect of substrate concentration: Peroxidases such as horseradish peroxidase (HRP)[50] catalyze the oxidation of substrates by hydrogen peroxide by way of a multi-step mecha-

nism. In the case of the single-electron substrate phenol used in this work, the net reaction is given by Equation (3).

$$H_2O_2 + 2\,\text{phenol} \xrightarrow{HRP} 2\,\text{phenoxy radicals} + 2\,H_2O \qquad (3)$$

As a result, hydrogen peroxide (HP) is catalytically decomposed by POx, and the two phenoxy radicals formed undergo dimerization (and possibly other reactions). From a mechanistic point of view, it is important to keep in mind that such assays work best if the concentration of the second substrate (phenol) is much higher than that of the hydrogen peroxide, since only under these conditions can the activity of POx be determined from the consumption of HP. No significant change in the fluorescence of the Eu_3TC–HP system was observed if the phenol concentration was kept below 3.5 mmol L^{-1}.

Optimization of the POx assay: Any change in pH will have two effects on the system. The first is on tetracycline, which has several dissociable groups that are also binding sites for metal ions.[51] The absorption and emission spectra of both tetracycline (TC) and its complex with Eu^{3+} are highly sensitive to pH.[22,44,45] The maximum enhancement of the fluorescence intensity on addition of HP occurs at pH 6.9 (a pH in the range 6.2–7.8 is suitable). The second effect concerns the enzyme. POx is rather robust and displays fairly strong activity in the pH range of 5–10.[50,52] A pH of 6.9 was chosen for further experiments since this results in a fairly strong fluorescence of Eu_3TC–HP at an acceptable level of enzyme activity.

The buffer systems MOPS, HEPES, Tris, and phosphate were tested in the assay. The MOPS buffer was found to be the most suitable, while HEPES was seen to have a slight quenching effect. Phosphate was found to interfere strongly, with a concentration of 12 μmol L^{-1} causing a quenching of the fluorescence of Eu_3TC by 21%. Tris buffer was found not to significantly affect the fluorescence; however, its best buffer capacity is between pH 7.5 and 9.0, which is somewhat outside of our preferred pH range. Therefore, a 10 mmol L^{-1} MOPS buffer at pH 6.9 was used in the following experiments.

Although the optimum temperature for POx is between 40 and 50 °C,[52] we chose 30 °C as the incubation temperature, since this gave satisfactory results in the monitoring of kinetic assays. Higher temperatures may conceivably be applied in certain cases or if shorter reaction times are desired. The fluorescence intensities of Eu_3TC and Eu_3TC–HP decrease strongly with increasing temperature. Interferences by common cations and anions were studied and no significant effects were found other than those of the common buffer ions phosphate and citrate. The POx–HP system itself is known to be prone to interference by ascorbic acid, uric acid, and bilirubin, as reported elsewhere.[52]

Time-resolved kinetic assay: Owing to the long decay times of the fluorescences of practically all europium complexes, they are often used in time-resolved fluorescent assays, which can effectively eliminate background features such as the intrinsic but short-lived fluorescence of proteins and that of plastic substrates such as micro-well plates. The assay presented here also enables a reduction in the background fluorescence of Eu_3TC (formed from Eu_3TC–HP) because the average decay times differ considerably (30 and 60 μs, respectively). From the decay profile and the experimental optimization, a lag time of 60 μs and an integration time of 40 μs were found to be most appropriate for the assay. No significant improvement was found when the integration time was increased from 40 to 100 μs. For the determination of high activities of POx, a 10 min incubation time proved to be adequate. The time-gated assay offers a dynamic range from 4.0×10^{-5} to 5.9×10^{-3} U mL^{-1}, with a limit of detection (LOD; at $S/N = 3$) of 1.0×10^{-5} U mL^{-1} after incubating for 50 min. In the case of the steady-state intensity assay, the dynamic range is slightly shifted to higher values, being between 8.5×10^{-5} and 4.5×10^{-2} U mL^{-1}, and with an LOD of 7.0×10^{-5} U mL^{-1} after incubating for 10 min.

Inhibitors of peroxidase: Cyanide is a strong and reversible inhibitor of POx.[50] It binds to the free sixth coordination site of the central iron(III) ion of the catalytic center of POx, that is, the one not occupied by the heme ligand. This, of course, is the same site as is involved in H_2O_2 binding, and thus cyanide binding retards or prevents the catalytic cycle.[53,54] In order to demonstrate this inhibition, Figure 3 shows the changes in the kinetics due to inhibition of POx, as monitored by means of the Eu_3TC–HP system. Curve A shows a time trace for a system in which cyanide was added to the Eu_3TC–HP/phenol mixture, but in the absence of POx. The fluorescence of Eu_3TC–HP remains unaffected by the cyanide. Curve E shows the uninhibited kinetics, while curves B, C, and D demonstrate that the activity of POx is inhibited if cyanide is present at a concentration of

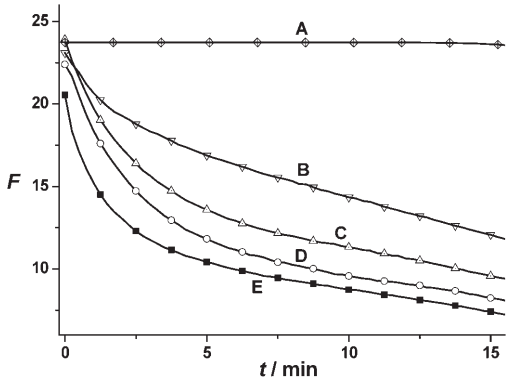

Figure 3. Effect of cyanide on the activity of POx, as monitored with the indicator Eu_3TC–HP in the presence of phenol: A) cyanide was added to the system (50 μL of Eu_3Tc stock solution, 20 μL of 4 mmol L^{-1} H_2O_2, and 17 μL of 49 mmol L^{-1} phenol, diluted with MOPS to a total volume of 250 μL) in the absence of POx; B)–D) responses in the presence of 0.2 U mL^{-1} of POx and cyanide at final concentrations of 440, 67, and 2.2 μmol L^{-1}, respectively; (E) response after addition of 0.2 U mL^{-1} of POx in the absence of cyanide.

2.2 μmol L^{-1} or higher. These results indicate that: a) the rate of decomposition of H_2O_2 by POx decreases with increasing cyanide concentration, and b) the probe can be used to quantify cyanide through inhibition of the activity of POx. Other known inhibitors of POx, such as sodium azide, interact with the Eu_3TC–HP system in the same manner as cyanide. Hydroxylamine, in contrast, exerts a quenching effect on the fluorescence of Eu_3TC-HP even in the absence of POx.

Time-resolved fluorimetric enzyme-linked immunosorbent assay (TRF-ELISA): Due to the reversible nature of the underlying chemistry, several kinds of enzymes may be employed in this ELISA method. These include catalases, peroxidases, and oxidases, all of which may be used as labels for antibodies. In a sandwich ELISA experiment (see Experimental Section), the wells of a 96-well microtiter plate were coated with rabbit anti-bovine IgG as the immobilized capture probe. After blocking of the residual surface of the wells with BSA, the immobilized anti-bovine IgG was first exposed to bovine IgG as the target antigen and then exposed to rabbit anti-bovine IgG/POx conjugate as the detector molecule.

After addition of solutions of Eu_3Tc, H_2O_2, and phenol, the decrease in fluorescence with time was recorded at a lag time of 60 μs after pulsed excitation. The integration time was set at 40 μs. Figure 4A shows the resulting normalized calibration plot for the linear range, which was obtained by plotting the normalized fluorescence $[(F_0-F)/F_0]$ versus the concentration of IgG. The LOD is as little as 0.1 ng mL^{-1} of IgG. The linear range is from 0.1 to 8.0 ng mL^{-1}, and standard deviations between identical spots are below 5%. Figure 4B shows the dynamic range of the ELISA up to concentrations of 600 ng mL^{-1} of IgG as a logarithmic plot. At concentrations higher than 10 ng mL^{-1}, near saturation of the signal response is achieved.

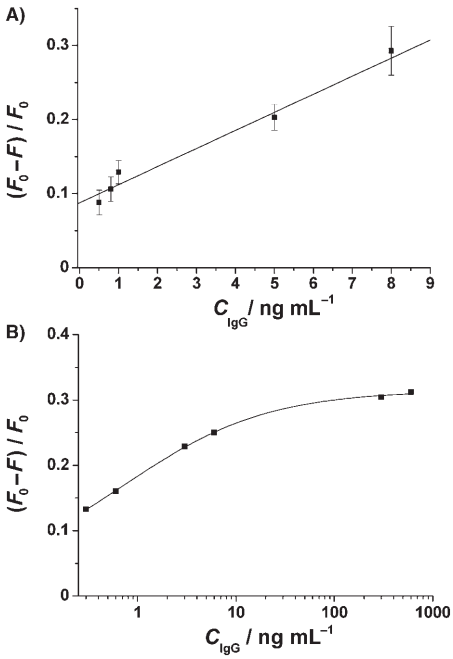

Figure 4. Referenced calibration graphs of the TRF-ELISA for IgG, as obtained by plotting $[(F_0-F)/F_0]$ versus the concentration of added bovine IgG. F_0 is the time-resolved fluorescence obtained in the absence of IgG after addition of POx-conjugated anti-bovine IgG and indicator solution containing Eu_3TC, H_2O_2, and phenol. In plot A), only the linear range is shown. The error bars represent the standard deviations as calculated from three spots of equal concentration. B) The logarithmic plot shows the overall dynamic range of the assay.

Time-resolved fluorescence imaging of an enzyme-linked immunosorbent assay: Conventional fluorescence readers analyze the wells of a microplate one by one. Faster screening is accomplished if all spots are excited and read simultaneously by means of fluorescence imaging. Given the advantages of the TRF-ELISA described above, we have adapted this scheme to imaging. The device used[23] consists of an array of 96 purple LEDs (λ_{max} = 405 nm) that excites the fluorescence of Eu_3TC–HP. The resulting emission is recorded by a CCD camera with the help of a light-guiding adapter consisting of 96 optical fibers. A schematic of the time course when acquiring TRF data is shown in Figure 6 in the Experimental Section.

The read-out of the time-resolved fluorescence imaging ELISA (TRFI-ELISA) for IgG was acquired after a 30 min incubation of the Eu_3TC–HP probe at room temperature. The result is shown in Figure 5 (in pseudocolors that reflect intensity). The dynamic range of this TRFI-ELISA is from 5 to 100 ng mL^{-1} for IgG. At high concentrations of IgG, complete decomposition of the Eu_3TC–HP complex is evident.

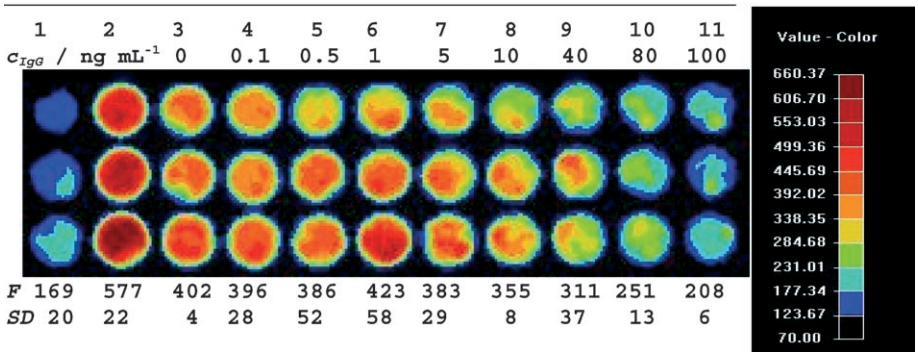

Figure 5. Pseudocolor fluorescence image of part of a micro-well plate containing the sandwich ELISAs for IgG. IgG concentrations range from 0 to 100 ng mL^{-1} (spot rows 3–11). Reference spot rows 1 (Eu_3TC only) and 2 (Eu_3TC–HP-phenol only) illustrate the upper and lower limits of the dynamic range. *F* is the relative intensity as calculated from an ROI in the centers of the spots (average of three spots of equal concentration). *SD* is the average standard deviation within the ROIs.

Fluorescence intensities were calculated and averaged considering regions of interest (ROIs) from the centers of the spots. The standard deviations between three different spots with the same IgG concentration were all of the same magnitude (between 5 and 10%).

It is obvious that imaging ELISA is advantageous in allowing fast data acquisition along with concise data visualization. This also makes the method suitable for high-throughput screening applications. The sensitivity of the imaging device may be further improved by making use of CCDs with longer signal integration times, by employing excitation sources with higher intensities, and by the use of more sophisticated optical set-ups.

Comparison with known methods for fluorimetric POx assays and POx-based ELISAs: Since H_2O_2 is not directly detectable by an optical signal (which is in contrast to electrochemical detection), substantial efforts have been made to identify chromogenic, fluorogenic, and luminogenic second substrates for the determination of the activity of POx. Fluorogenic substrates include homovanillic acid,[26] *p*-hydroxyphenylacetic acid,[30] *p*-hydroxyphenylpropionic acid,[31] and Amplex Red.[55] Recently, new substrates such as 4-(*N*-methylhydrazino)-7-nitro-1,2,3- benzoxadiazole[56] and 10-methylacridane-9-carboxyhydrazide[57] have been presented (Table 1). In practice, none of them can be exploited for the time-resolved determination of POx. Although the enzyme-amplified lanthanide luminescence (EALL) method had been known for almost two decades, it was not used in POx assays until Meyer and Karst[39] found that a fluorescent ternary complex is formed between Tb^{3+}, EDTA, and the oxidation product formed by the action of POx on *p*-hydroxyphenylpropionic acid. This complex has a decay time of about 100 μs, thus possibly enabling time-resolved determination, and works best in the presence of an enhancer such as CsCl.

The optical ELISA methods that have been described to date have been mainly based on the quantification of an oxidation product generated by POx. The one described here is based on the direct and non-enzymatic determination of residual hydrogen peroxide (HP) using a probe that is fairly specific for this molecule. Such a probe has not been reported previously. Since the activity of the POx is affected by the second substrate,[28,29] the detection of the HP consumed offers advantages over methods based on determination of the oxidation products of second substrates.

In contrast to existing POx-ELISAs (see Table 2), which utilize a second substrate that is converted into a detectable species, the assay presented here makes use of a fluorescent and direct probe for HP, does not require the addition of enhancers, works best at neutral pH, and can be applied to both intensity-based and time-resolved determinations. Despite not having been optimized, this ELISA gives an LOD that is comparable with those obtained with common micro-

Table 1. Figures of merit for comparable fluorimetric assays for POx.

	Method	ex/em [λ]/[nm]	LODs	Analytical (or linear) range	Ref.
1	homoovanillic acid (HVA)	315/425	1 mU	1–10 mU	[26,30]
2	tyramine	326/410	500 μU	0.5–10 mU	[27,31]
3	3-(*p*-hydroxyphenyl)propionic acid (HPPA)	320/404	7.8 μU	7.8 μU–1 mU	[31]
4	*p*-hydroxyphenethyl alcohol (*p*-tyrosol)	320/404	15.6 μU	0.016–1 mU	[31]
5	*N,N′*-dicyanomethylene-*o*-phenylenediamine (DCM-OPA)	255,334, 353/455		21–150 pmol L^{-1}	[60]
6	10-methylacridane-9-carboxylate hydrazide	357/510	0.046 pmol L^{-1}		[57]
7	10-acetyl-3,7-dihydroxyphenoxazine (Amplex Red)	563/587	10 μU mL^{-1}	0.0–2 mU mL^{-1}	[55]
8	4-(*N*-methylhydrazino)-7-nitro-2,1,3-benzoxadiazole (MNBDH)	470/547	22 nM for H_2O_2 (POx-catalyzed)		[56]
9	tetrasubstituted amino aluminum phthalocyanine	610/678	0.59 pmol L^{-1}	0–40 pmol L^{-1}	[61]
10	oxidation of *p*HPPA-Tb^{III}-EDTA, addn. of CsCl	320/545	2 pmol L^{-1}	2 pmol L^{-1}–10 nmol L^{-1}	[39]
11	Eu_3Tc-HP	390–410/618	10 μU mL^{-1}	0.04–5.9 mU mL^{-1}	this method

Table 2. Figures of merit for commonly used and commercial kits and reagents for ELISA.

Method	Reagent(s)	abs(exc)/em [λ]/[nm][a]	Analyte	LOD	Analytical range	Comments	Ref.
fluorogenic substrate	Amplex UltraRed	568/581	C-reaction protein	75 pg mL^{-1}		more sensitive; small Stokes' shift	[55]
chromogenic substrate	3,3′,5,5′-tetramethyl-benzidine	450/–	albumin	30 ng mL^{-1}	0.05–5 μg mL^{-1}	prone to oxidation; limited water solubility	[46]
DELFIA[b]	Eu-2 (ligand)$_3$	340/615	anti-tetanus antibodies	3 μU mL^{-1}	0.3–100 000 mU mL^{-1}	two-step protocol; no amplification by enzyme; large linear range; has the merits of lanthanide probes	[16]
fluorescent Eu probe[c]	Eu_3Tc-HP	405/616	IgG	0.1 ng mL^{-1}	0.1–8 ng mL^{-1}	combines the merits of enzyme amplification and lanthanide probes; more sensitive	this work

[a] abs, exc, and em denote absorption, fluorescence excitation, and fluorescence emission maxima, respectively. [b] DELFIA: dissociation-enhanced lanthanide fluorescent immunoassay. [c] Data for the time-resolved sandwich POx-ELISA.

plate fluorescence readers described in the literature (see Table 1). The method presented here is fundamentally different from other time-resolving methods that use europium chelates as labels for secondary antibodies.[58,59] As a result, it is considered to be an attractive novel scheme for both assays of POx activity and POx-based ELISAs.

Conclusion

A method for determining the activity of POx through its H_2O_2 consumption at neutral pH has been demonstrated, which makes use of the fluorescent probe Eu_3Tc-HP. This lanthanide complex provides a convenient and sensitive assay for determination of the free enzyme and of POx conjugated to antibodies as used in ELISAs. It displays the typical virtues of lanthanide luminescence, including a large Stokes' shift, a line-like emission, and μs decay times that allow the suppression of background fluorescence through TRF detection. This fluorescent probe can be excited with a blue LED of wavelength 405 nm. Thereby, bioassays can be performed using the metal-ligand complex as indicator by means of either fluorescence intensity or decay time measurements. The latter scheme can be applied to fluorescence imaging, with its specific features of fast data acquisition and direct data visualization. A simple time-resolving imaging device has been developed, which was adjusted to the optical properties of the europium complex used as indicator. As the europium probe is generally not specific towards a particular analyte and the presence of other enzymes such as catalase can interfere with the presented assay, it is not suitable for the analysis of medical samples such as blood serum. Rather, this system has potential in high-throughput type assays (e.g., in the screening of enzyme inhibitors or activators) or in proteomic screening and immunoassays performed in ELISA format.

Experimental Section

Apparatus: Absorption spectra were acquired on a Cary WinUV spectrophotometer (Varian, Victoria, Australia; www.varianinc.com). Fluorescence studies of the effects of H_2O_2 (HP) and phenol on the spectra of Eu_3TC and Eu_3TC–HP were performed on an SLM AB2 luminescence spectrometer (Spectronic Unicam, Rochester, New York, USA; www.thermospectronic.com). Fluorescence intensity and kinetic data were acquired on either a Fluoroskan Ascent microtiter plate reader (from Thermo Labsystems, Helsinki, Finland; www.labsystems.com) or on a Tecan GENios+ micro plate reader (Tecan, Groedig, Austria; www.tecan.com). The excitation/emission filters were set to either 405/620 nm or 405/612 nm (other wavelengths are not available on these instruments; the emission maximum of the Eu_3TC complex is at 616 nm). Time-resolved fluorescence intensities were also measured by means of the GENios reader. The 96-well microtiter plates were obtained from Greiner Bio-One GmbH (Frickenhausen, Germany; www.greiner-lab.com).

Reagents: Peroxidase (EC 1.11.1.7., type I, from horseradish, 148 $U\,mg^{-1}$ solid) was purchased from Sigma (Deisenhofen, Germany; www.sigmaaldrich.com). The activity unit used here is based on the definition given by the producer: one unit will form 1.0 mg of purpurogallin from pyrogallol in 20 s at pH 6.0 at 20 °C. Rabbit anti-bovine IgG, bovine IgG, and rabbit anti-bovine IgG-peroxidase conjugate (all from Sigma) were diluted to the respective working concentrations with PBS. All inorganic salts were obtained in analytical grade purity from Merck (Darmstadt, Germany; www.merckeurolab.com) unless otherwise stated. Solutions were prepared in $10\,mmol\,L^{-1}$ 3-(*N*-morpholino)propanesulfonic acid (MOPS) buffer at pH 6.9 (Roth, Karlsruhe, Germany; www.carl-roth.de), except for IgG and anti-IgG, which were diluted with a PBS buffer at pH 7.4. Note that after using PBS, the phosphate of which may quench the fluorescence of Eu_3TC, needs to be washed out with MOPS buffer before adding the Eu_3TC solution. Phosphate-buffered saline (PBS) was obtained by dissolving KH_2PO_4 (0.26 g), $Na_2HPO_4{\cdot}7\,H_2O$ (2.17 g), and NaCl (8.71 g) in distilled water (900 mL), adjusting the solution to pH 7.4 with $1.0\,mol\,L^{-1}$ HCl or NaOH, and making up the volume to 1 L. High-purity hydrogen peroxide (H_2O_2) was purchased as a 30% solution from Merck. Europium(III) trichloride hexahydrate was obtained from Alfa Products (Danvers, USA; www.alfa.com), tetracycline hydrochloride from Serva (Heidelberg, Germany; www.serva.de). Tris(hydroxymethyl)aminomethane (Tris) and 4-(2-hydroxyethyl)piperazine-1-ethanesulfonic acid (HEPES) were purchased from Sigma-Aldrich.

A stock solution of Eu_3TC was prepared by mixing 10 mL of a $6.3\,mmol\,L^{-1}$ solution of $EuCl_3$ with 10 mL of a $2.1\,mmol\,L^{-1}$ solution of tetracycline hydrochloride and then diluting to 100 mL with MOPS buffer. This reagent is available from Chromeon (Regensburg, Germany; www.chromeon.com) and may be diluted to the concentration required. A fresh $5\,mmol\,L^{-1}$ solution of hydrogen peroxide in MOPS buffer was prepared every day. A $0.5\,mol\,L^{-1}$ phenol solution was stored at 4 °C and was diluted as required.

Calibration of the POx assay: Eu_3TC stock solution (20–50 μL), $5\,mmol\,L^{-1}$ H_2O_2 solution (20 μL), and $50\,mmol\,L^{-1}$ phenol solution (17 μL) were placed in each well of a thermostatted (30 °C) 96-well microtiter plate and MOPS buffer was added to give a final volume of 250 μL per well. After 10 min, POx solutions with activities ranging from 4.0×10^{-5} to $4.5\times10^{-2}\,U\,mL^{-1}$ were added, and the decrease in the time-resolved fluorescence intensity was recorded, typically over 5–60 min, depending on the activity of the POx. The lag time was set at 60 μs, and the integration time at 40 μs.

ELISA protocol for the detection of bovine IgG

1) Immobilization of anti-IgG in the wells of microtiter plates: Aliquots (200 μL) of rabbit anti-bovine-IgG at a concentration of $5\,\mu g\,mL^{-1}$ in 10 mM PBS (pH 7.4) were added to each well of the microtiter plate, which was then incubated at 37 °C for 1 h. Alternatively, it could be incubated at 4 °C overnight. Thereafter, the plate was rinsed twice with PBS.

2) Blocking of remaining binding sites: 200 μL of 1% BSA in $10\,mmol\,L^{-1}$ PBS (pH 7.4) was added to each well and the plate was incubated at 37 °C for 30 min. It was then rinsed twice with PBS.

3) Sample loading: Aliquots (200 μL) of different concentrations of bovine IgG were added to each well and the plate was incubated at 37 °C for 1 h. It was then rinsed twice with PBS buffer.

4) Coating with secondary antibody (POx-labeled): Aliquots (200 μL) of rabbit anti-bovine IgG-POx conjugate were added to each well at a concentration of 1:1500 (as recommended by the manufacturer) and the plate was incubated at 37 °C for 1 h. It was then rinsed twice with MOPS buffer to remove any PBS.

5) Detection: Solutions of Eu_3Tc, H_2O_2, and phenol were added to the wells (as described in the recommended POx protocol) and fluorescence readings were taken over time.

Imaging: The imaging system set-up consists of a fast gateable CCD camera (SensiMode; from PCO, Kelheim, Germany; see: www.pco.de), a pulsable LED array with 96 UV light-emitting diodes (λ_{max} = 405 nm; Roithner Laser Technik, Vienna, Austria; see: www.roithner-laser.com), a 96-fiber light-guiding adapter, a pulse generator (DG 535, Scientific Instruments GmbH, Gilching, Germany; see: www.si-gmbh.de), optical filters for excitation (BG 12; Schott) and emission (KV 550; Schott), and a personal computer for controlling the experiments and visualization of the micro-well arrays. The device and the pulsed data acquisition process along with the corresponding software modules have been described else-

where.[23] The images were processed, visualized, and evaluated with the IDL software module (Research Systems, Inc., Boulder, CO; see: www.rsinc.com).

The camera was gated during the exposure by an external trigger signal, as shown schematically in Figure 6. The excitation pulse had a width of

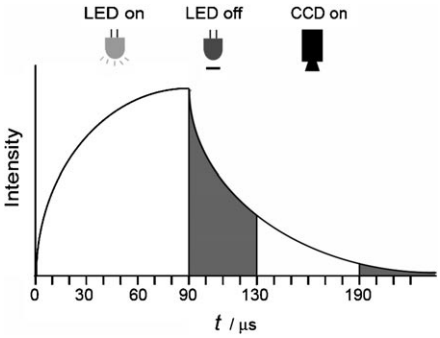

Figure 6. Time course of a single pulsed excitation and time-resolved acquisition cycle in time-resolved fluorescence imaging (TRFI).

90 µs, the lag time was set at 40 µs, the integration time was set at 60 µs, and the detection window was open in the time interval 130–190 µs after starting the LED pulse. The resulting image is a superimposition of several single pictures. The corresponding background images were recorded in a second acquisition cycle within the same time gates without prior excitation and finally subtracted from the emission signals. The whole imaging process for the read-out of a microtiter plate was accomplished using three consecutive acquisition cycles for data evaluation and quantification.

Time-correlated single-photon counting (TCSPC) lifetime determination: The luminescence decay profiles of EuTc and EuTc-HP were detected with a pulsed 392 nm laser (LDH-C-400, PicoQuant GmbH, Berlin, Germany; www.picoquant.de) in combination with an H5783-P04 PMT detector (Hamamatsu) with a newly developed multiphoton-counting board in a special multipass cuvette. The samples were prepared by addition of different concentrations (0–300 µmol L^{-1}) of H_2O_2 to a final concentration of EuTc of 53.3 µmol L^{-1}. Measurements were made after waiting for 10 min. Data were processed with FluoFit software (from PicoQuant GmbH).

Acknowledgements

We thank Dr. Jörg Enderlein (FZ Jülich) and Henrik Bauer (PicoQuant GmbH, Berlin) for the determination of decay times. M.W. and Z.L. thank Chromeon GmbH for financial support.

[1] a) C. Yang, L. M. Fu, Y. Wang, J.-P. Zhang, W.-T. Wong, X.-C. Ai, Y.-F. Quiao, B.-S. Zou, L.-L. Gui, *Angew. Chem.* **2004**, *116*, 5120–5123; *Angew. Chem. Int. Ed.* **2004**, *43*, 5010–5013.
[2] F. J. Steemers, W. Verboom, D. N. Reinhoudt, E. B. van der Tol, J. W. Verhoeven, *J. Am. Chem. Soc.* **1995**, *117*, 9408–9414.
[3] A. M. Klonkowski, S. Lis, M. Pietraszkiewicz, Z. Hnatejko, K. Czarnobaj, M. Elbanowski, *Chem. Mater.* **2003**, *15*, 656–663.
[4] P. S. Peijzel, A. Meijerink, R. T. Wegh, M. F. Reid, G. W. Burdick, *J. Solid State Chem.* **2005**, *178*, 448–453.
[5] M. A. Kessler, *Anal. Chim. Acta* **1998**, *364*, 125–129.
[6] C. Cano-Raya, M. D. Fernández Ramos, L. F. Capitán Vallvey, O. S. Wolfbeis, M. Schäferling, *Appl. Spectrosc.* **2005**, *59*, 1209–1216.
[7] R. Ziessel, L. J. Charbonniere, *J. Alloys Compd.* **2004**, *374*, 283–288.
[8] R. A. Poole, G. Bobba, M. J. Cann, J.-C. Frias, D. Parker, R. D. Peacock, *Org. Biomol. Chem.* **2005**, *3*, 1013–1024.
[9] R. S. Dickins, S. Aime, A. S. Batsanov, A. Beeby, M. Botta, J. I. Bruce, J. A. K. Howard, C. S. Love, D. Parker, R. D. Peacock, H. Puschmann, *J. Am. Chem. Soc.* **2002**, *124*, 12697–12705.
[10] a) Z. Lin, M. Wu, M. Schäferling, O. S. Wolfbeis, *Angew. Chem.* **2004**, *116*, 1767–1770; *Angew. Chem. Int. Ed.* **2004**, *43*, 1735–1738.
[11] a) O. S. Wolfbeis, A. Dürkop, M. Wu, Z. Lin, *Angew. Chem.* **2002**, *114*, 4681–4684; *Angew. Chem. Int. Ed.* **2002**, *41*, 4495–4498.
[12] J. Meyer, U. Karst, *Analyst* **2001**, *126*, 175–178.
[13] E. F. Templeton, H. E. Wong, R. A. Evangelista, T. Granger, A. Pollak, *Clin. Chem.* **1991**, *37*, 1506–1512.
[14] I. Hemmila, *Immunochemistry* **1997**, *1*, 193–214.
[15] E. Toivonen, I. Hemmila, J. Marniemi, P. N. Joergensen, J. Zeuthen, T. Loevgren, *Clin. Chem.* **1986**, *32*, 637–640.
[16] E. Merkela, T. H. Stahlberg, I. Hemmila, *J. Immunol. Methods* **1993**, *161*, 1–6.
[17] K. Kuningas, T. Rantanen, U. Karhunen, T. Loevgren, T. Soukka, *Anal. Chem.* **2005**, *77*, 2826–2834.
[18] Y. X. Ci, Y. Z. Li, X. J. Liu, *Anal. Chem.* **1995**, *67*, 1785–1788.
[19] R. Liu, J. Yang, X. Wu, *J. Lumin.* **2002**, *##33##96*, 201–209.
[20] C. Jiang, L. Luo, *Anal. Chim. Acta* **2004**, *506*, 171–175.
[21] J. Chongqiu, L. Li, *Anal. Chim. Acta* **2004**, *511*, 11–16.
[22] Y. Rakicioglu, J. H. Perrin, S. G. Schulman, *J. Pharm. Biomed. Anal.* **1999**, *18*, 397–399.
[23] M. Schäferling, M. Wu, J. Enderlein, H. Bauer, O. S. Wolfbeis, *Appl. Spectrosc.* **2003**, *57*, 1386–1392.
[24] M. Wu, Z. Lin, O. S. Wolfbeis, *Anal. Biochem.* **2002**, *320*, 129–135.
[25] M. Wu, Z. Lin, M. Schäferling, A. Duerkop, O. S. Wolfbeis, *Anal. Biochem.* **2005**, *340*, 66–73.
[26] G. G. Guilbault, P. J. Brignac Jr., M. Zimmer, *Anal. Chem.* **1968**, *40*, 190–196.
[27] http://www.unige.ch/LABPV/perox.html
[28] J. N. Rodriguez-Lopez, A. T. Smith, R. N. F. Thorneley, *J. Biol. Chem.* **1996**, *271*, 4023–4030.
[29] P. D. Josephy, T. Eling, R. P. Mason, *J. Biol. Chem.* **1982**, *257*, 3669–3675.
[30] G. G. Guilbault, P. J. Brignac Jr., M. Juneau, *Anal. Chem.* **1968**, *40*, 1256–1263.
[31] K. Zaitsu, Y. Ohkura, *Anal. Biochem.* **1980**, *109*, 109–113.
[32] A. N. Diaz, F. G. Sanchez, J. A. G. Garcia, V. B. del Rio, *J. Biolumin. Chemilumin.* **1995**, *10*, 285–289.
[33] L. J. Kricka, X. Ji, *Anal. Sci.* **1991**, *7*, 1501–1506.
[34] Y. A. Vladimirov, V. S. Sharov, T. B. Suslova, *Photobiochem. Photobiophys.* **1981**, *2*, 279–284.
[35] C. A. Marquette, L. J. Blum, *Sens. Actuators B* **1998**, 51, 100–106.
[36] M. Darder, K. Takada, F. Pariente, E. Lorenzo, H. D. Abruna, *Anal. Chem.* **1999**, *71*, 5530–5537.
[37] A. Morrin, A. Guzman, A. J. Killard, J. M. Pingarron, M. R. Smyth, *Biosens. Bioelectron.* **2003**, *18*, 715–720.
[38] E. F. Gudgin Dickson, A. Pollak, E. P. Diamandis, *J. Photochem. Photobiol. B* **1995**, *27*, 3–19.
[39] J. Meyer, U. Karst, *Analyst* **2000**, *125*, 1537–1538.
[40] J. Little, *Enzyme Labeled Immunoassay, in Immunoassay* (Ed.: R. Edwards), Wiley, Chichester, **1996**, pp. 47–62.
[41] I. Durrant, *Direct peroxidase labelling of hybridisation probes and chemiluminescence detection, in Nonradioactive Analysis of Biomolecules,* 2nd ed. (Eds.: C. Kessler), Springer, Heidelberg, **2000**, chap. 12, pp. 206–213.
[42] G. R. Nakayama, *Curr. Opin. Drug Discovery Dev.* **1998**, *1*, 85–91.
[43] E. J. M. Speel, A. H. N. Hopman, P. Komminotha, *J. Histochem. Cytochem.* **1999**, *47*, 281–288.
[44] L. M. Hirschy, T. F. Van Geel, J. D. Winefordner, R. N. Kelly, S. G. Schulman, *Anal. Chim. Acta* **1984**, *166*, 207–219.
[45] H. X. Li, J. J. Zhang, X. W. He, G. J. Li, *Chin. J. Chem.* **2004**, *22*, 177–183.
[46] X. R. Chen, Y. T. Chen, S. F. Shen, *J. Immunoassay Immunochem.* **2004**, *25*, 81–89.
[47] F. S. Richardson, *Chem. Rev.* **1982**, *82*, 541–552.
[48] D. Parker, R. S. Dickins, H. Puschmann, C. Crossland, J. A. K. Howard, *Chem. Rev.* **2002**, *102*, 1977–2010.

[49] W. Lei, A. Dürkop, Z. Lin, M. Wu, O. S. Wolfbeis, *Microchim. Acta* **2003**, *143*, 269–274.
[50] H. B. Dunford, *Horseradish peroxidase: structure and kinetic properties, in Peroxidases in Chemistry and Biology, vol. II* (Eds.: J. Everse, K. E. Everse, M. B. Grisham), CRC Press, Boca Raton, **1991**, pp. 1–24.
[51] H. L. A. Duarte, S. Carvalho, E. B. Paniago, A. M. Simas, *J. Pharm. Sci.* **1999**, *88*, 111–120.
[52] D. Schomburg, D. Stephan, *Enzyme Handbook*, Springer, Berlin, Heidelberg, **1994**.
[53] J. S. de Ropp, P. K. Mandal, G. N. La Mar, *Biochemistry* **1999**, *38*, 1077–1086.
[54] A. Henriksen, A. T. Smith, M. Gajhede, *J. Biol. Chem.* **1999**, *274*, 35005–35011.
[55] R. Haugland, *Handbook of fluorescent probes and research chemicals*, Molecular Probes Inc.; http://www.probes.com.
[56] a) J. Meyer, A. Büldt, M. Vogel, U. Karst, *Angew. Chem.* **2000**, *112*, 1510–1512; *Angew. Chem. Int. Ed.* **2000**, *39*, 1453–1455.
[57] H. Akhavan-Tafti, R. de Silva, R. Eickholt, R. Handley, M. Mazelis, M. Sandison, *Talanta* **2003**, *60*, 345–354.
[58] P. Huhtinen, M. Kivelä, O. Kuronen, V. Hagren, H. Takalo, H. Tenhu, T. Loevgren, H. Härmä, *Anal. Chem.* **2005**, *77*, 2643–2648.
[59] K. Kunigas, T. Rantanen, U. Karhunen, T. Loevgren, T. Soukka, *Anal. Chem.* **2005**, *77*, 2826–2834.
[60] Y. Li, H. Liu, Z. Dong, W. Chang, Y. Ci, *Microchem. J.* **1996**, *53*, 428–436.
[61] X. Chen, H. Yang, Q. Zhu, H. Zheng, J. Xu, D. Li, *Analyst* **2001**, *126*, 523–527.

Received: July 26, 2005
Revised: November 8, 2005
Published online: January 17, 2006

